



**HAL**  
open science

## **Auroral Storm and Polar Arcs at Saturn-Final Cassini/UVIS Auroral Observations**

B. Palmaerts, A. Radioti, D. Grodent, Z. Yao, T. Bradley, E. Roussos, L.  
Lamy, E. Bunce, S. Cowley, N. Krupp, et al.

► **To cite this version:**

B. Palmaerts, A. Radioti, D. Grodent, Z. Yao, T. Bradley, et al.. Auroral Storm and Polar Arcs at Saturn-Final Cassini/UVIS Auroral Observations. *Geophysical Research Letters*, 2018, 45 (14), pp.6832-6842. 10.1029/2018GL078094 . hal-02344519

**HAL Id: hal-02344519**

**<https://hal.science/hal-02344519>**

Submitted on 18 Nov 2021

**HAL** is a multi-disciplinary open access archive for the deposit and dissemination of scientific research documents, whether they are published or not. The documents may come from teaching and research institutions in France or abroad, or from public or private research centers.

L'archive ouverte pluridisciplinaire **HAL**, est destinée au dépôt et à la diffusion de documents scientifiques de niveau recherche, publiés ou non, émanant des établissements d'enseignement et de recherche français ou étrangers, des laboratoires publics ou privés.

Copyright

## RESEARCH LETTER

10.1029/2018GL078094

## Special Section:

Cassini's Final Year: Science Highlights and Discoveries

## Key Points:

- An intense auroral storm indicates the occurrence of magnetotail reconnection induced by an ICME
- First observational evidence of the formation of a nightside polar arc
- Most polar auroral arc ever observed at Saturn

## Correspondence to:

B. Palmaerts,  
b.palmaerts@ulg.ac.be

## Citation:

Palmaerts, B., Radioti, A., Grodent, D., Yao, Z. H., Bradley, T. J., Roussos, E., et al. (2018). Auroral storm and polar arcs at Saturn—Final Cassini/UVIS auroral observations. *Geophysical Research Letters*, 45, 6832–6842. <https://doi.org/10.1029/2018GL078094>

Received 27 MAR 2018

Accepted 8 JUN 2018

Accepted article online 19 JUN 2018

Published online 27 JUL 2018

## Auroral Storm and Polar Arcs at Saturn—Final Cassini/UVIS Auroral Observations

B. Palmaerts<sup>1</sup> , A. Radioti<sup>1</sup>, D. Grodent<sup>1</sup> , Z. H. Yao<sup>1</sup>, T. J. Bradley<sup>2</sup> , E. Roussos<sup>3</sup> , L. Lamy<sup>4</sup> , E. J. Bunce<sup>2</sup> , S. W. H. Cowley<sup>2</sup> , N. Krupp<sup>3</sup> , W. S. Kurth<sup>5</sup> , J.-C. Gérard<sup>1</sup> , and W. R. Pryor<sup>6</sup> 

<sup>1</sup>Laboratoire de Physique Atmosphérique et Planétaire, Space Sciences, Technologies and Astrophysics Research Institute, Université de Liège, Liège, Belgium, <sup>2</sup>Department of Physics and Astronomy, University of Leicester, Leicester, UK, <sup>3</sup>Max-Planck-Institut für Sonnensystemforschung, Göttingen, Germany, <sup>4</sup>LESIA, Observatoire de Paris, Meudon, France, <sup>5</sup>Department of Physics and Astronomy, University of Iowa, Iowa City, IO, USA, <sup>6</sup>Science Department, Central Arizona College, Coolidge, AZ, USA

**Abstract** On 15 September 2017 the Cassini spacecraft plunged into Saturn's atmosphere after 13 years of successful exploration of the Saturnian system. The day before, the Ultraviolet Imaging Spectrograph (UVIS) on board Cassini observed Saturn's northern aurora for about 14 hr. During these observations, several auroral structures appeared, providing clues about processes simultaneously occurring in Saturn's magnetosphere. The observed dawn auroral enhancement together with the magnetic field and plasma wave data suggest that an intense flux closure process took place in the magnetotail. This enhanced magnetotail reconnection is likely caused by a magnetospheric compression induced by an interplanetary shock. Additionally, a polar arc is observed on the duskside, tracked for the first time from its growth until its quasi-disappearance and used as an indicator of reconnection location on the dayside magnetopause. Observation of an atypical auroral arc at very high latitudes supports the interplanetary shock scenario.

**Plain Language Summary** The plasma dynamics within Saturn's magnetosphere and the interactions of the plasma with the planetary magnetic field and the atmosphere are very complex. The magnetospheric dynamics can be investigated using the observations of the auroral emissions in the upper atmosphere of the polar regions of Saturn, since these polar lights are generated by precipitation into the atmosphere of electrons guided by the magnetic field lines. These electrons originating from various regions of the magnetosphere, the auroral emissions provide a global picture of the magnetospheric processes all around the planet. Here we use the final observations of Saturn's aurora by the Cassini spacecraft to understand the processes which occur in Saturn's magnetosphere on the day before the end of the Cassini mission in September 2017. In particular, a brightening and a broadening of one part of the aurora might be the response to a compression of the magnetosphere induced by an interplanetary shock in the solar wind. Additionally, an arc-like auroral structure was tracked for the first time from its growth until its disappearance, revealing the mechanism producing it. Finally, the aurora exhibits another arc almost at the pole which had never been observed before.

### 1. Introduction

Saturn's ultraviolet (UV) aurorae were initially observed by Pioneer 11 (Judge et al., 1980), Voyager (Broadfoot et al., 1981; Sandel & Broadfoot, 1981), and International Ultraviolet Explorer (IUE; Clarke et al., 1981; McGrath & Clarke, 1992) before being studied using images provided by different cameras and spectrographs on board the Hubble Space Telescope (HST; e.g., Gérard et al., 1995, 2004; Prangé et al., 2004; Trauger et al., 1998). The arrival of the Cassini spacecraft to the Saturnian system in July 2004 opened a new era of investigation of the UV aurorae glowing in Saturn's upper atmosphere since the Cassini Ultraviolet Imaging Spectrograph (UVIS; Esposito et al., 2004) was suitable for the observation of these auroral emissions.

Auroral studies during the Cassini mission have shown that Saturn's magnetosphere is governed by a combination of internally driven and solar wind-driven flux tube convection cycles (e.g., Badman et al., 2015; Grodent, 2015; Radioti, Grodent, Gérard, et al., 2017), as also suggested by magnetic field observations (Jackman et al., 2011) and theory (e.g., Badman & Cowley, 2007; Southwood & Chané, 2016). Since Saturn is a rapidly rotating planet and its environment is fed by internal plasma sources, mainly the icy moon Enceladus

(see the review by Blanc et al., 2015) plasma transport inside the magnetosphere is driven by internal processes, in particular, the Vasyliūnas cycle (Vasyliūnas, 1983). In this cycle, highly mass-loaded flux tubes are stretched out as they rotate around the planet toward the nightside and eventually pinch off through reconnection in the magnetotail. In the solar wind-driven cycle, also known as the Dungey cycle (Dungey, 1961), magnetic reconnection at the dayside magnetopause between the planetary field and the antiparallel component of the interplanetary magnetic field (IMF) adds open flux in the magnetosphere. Dragged by the solar wind, the open field lines convect to the nightside in the lobes. The open flux is subsequently closed through reconnection in the magnetotail and the newly closed field lines can convect back to the dayside.

The main auroral emission at Saturn consists of a ring of emissions around Saturn's poles, sometimes forming a spiral and often interrupted by discontinuities. The main emission is thought to be generated by upward field-aligned currents flowing along closed magnetic field lines near the boundary between the closed and the open field lines (Belenkaya et al., 2008; Bunce et al., 2008; Hunt et al., 2014, 2015; Jinks et al., 2014). As a consequence, the main emission is strongly controlled by the solar wind conditions, so that the arrival of a solar wind shock leads to a brightening and a poleward expansion of the main aurora in the dawn sector (e.g., Badman et al., 2005; Clarke et al., 2009; Grodent et al., 2005; Jia et al., 2012). This intense auroral activity, usually referred to as an *auroral storm* (e.g., Grodent et al., 2005; Meredith et al., 2014; Nichols et al., 2014; Prangé et al., 2004), is triggered by enhanced closure of magnetic flux through magnetotail reconnection (Cowley et al., 2005). Finally, Dungey-type tail reconnection in the absence of dayside reconnection can result in a buildup of closed flux in the tail and the development of a nightside polar arc (Radioti et al., 2014).

Some of the auroral structures briefly reviewed here are further discussed in the following sections where we present a long observation sequence of UV auroral emissions captured by Cassini/UVIS before the end of the mission.

## 2. Final Cassini/UVIS Auroral Observations

On 13 September 2017 (day of year, DOY 256) at 18:32 UT, two days before the final plunge of the Cassini spacecraft into Saturn's atmosphere, the UVIS spectrograph started to obtain the ultimate round of observations of the Kronian aurorae. During this observation period, which ended on 14 September (DOY 257) at 17:22 UT, Cassini was in the nightside magnetosphere, moving from 16.9 to 11.3  $R_S$  radial distance from the planet and from 16.6° to 25.8° in latitude. The northern auroral region was scanned 31 times by the UVIS slit using the FUV channel (111–191 nm), enabling us to follow the evolution of auroral features over about 23 hr. We here focus on the last 20 scans starting at 02:51 UT on day 257/2017.

The time required (~60 min) to sweep the whole auroral region with the UVIS slit leads to a significant time delay between the different rows of the acquired image. Because of this time delay within the UVIS images, they are sometimes referred to as *pseudoimages*. In the UVIS observations presented here, ~10 min were necessary to capture the whole auroral region (with an integration time of 16 s per row), except for the final image for which the duration of the scan was 60 min (60 s per row). The UVIS scans of the auroral region have been projected onto a polar plane fixed in local time using the method described by Grodent et al. (2011), and considering that the emissions peak at 1,100 km above the 1-bar pressure level (Gérard et al., 2009). The polar projections are displayed in Figure 1 as seen from above the north pole and oriented with the direction of the Sun to the bottom. The starting acquisition time is indicated at the top of each frame. In order to reveal as many auroral structures as possible along the sequence, the color scale evolves from one image to another. The intensity value in kiloRayleighs (kR) above which the color scale is saturated (red color) is indicated on each panel. Intensity values are obtained using the unabsorbed H<sub>2</sub> auroral spectrum (~1,400–1,600 Å; Gustin et al., 2017). For each image, the brightness distribution has been truncated at the 99th percentile in order to exclude the pixels with anomalous intensity values. The complete projection is shown on the left (A), while the dusk half of the polar projection, from noon to midnight, is reproduced on the right (B) with a saturated color table revealing the faintest emissions. The stretching of the pixels in the noon sector are due to the mapping of the emission close to the limb. These pixels were not considered in the following analysis. The trajectory of Cassini was magnetically mapped to the ionosphere (yellow line for day 257/2017 and red line for the UVIS observing time) by using the internal field model of Burton et al. (2010) combined with the ring current model of Bunce et al. (2007).

In the next sections, the auroral emission during the final UVIS observing sequence is described and discussed in the context of magnetospheric dynamics.

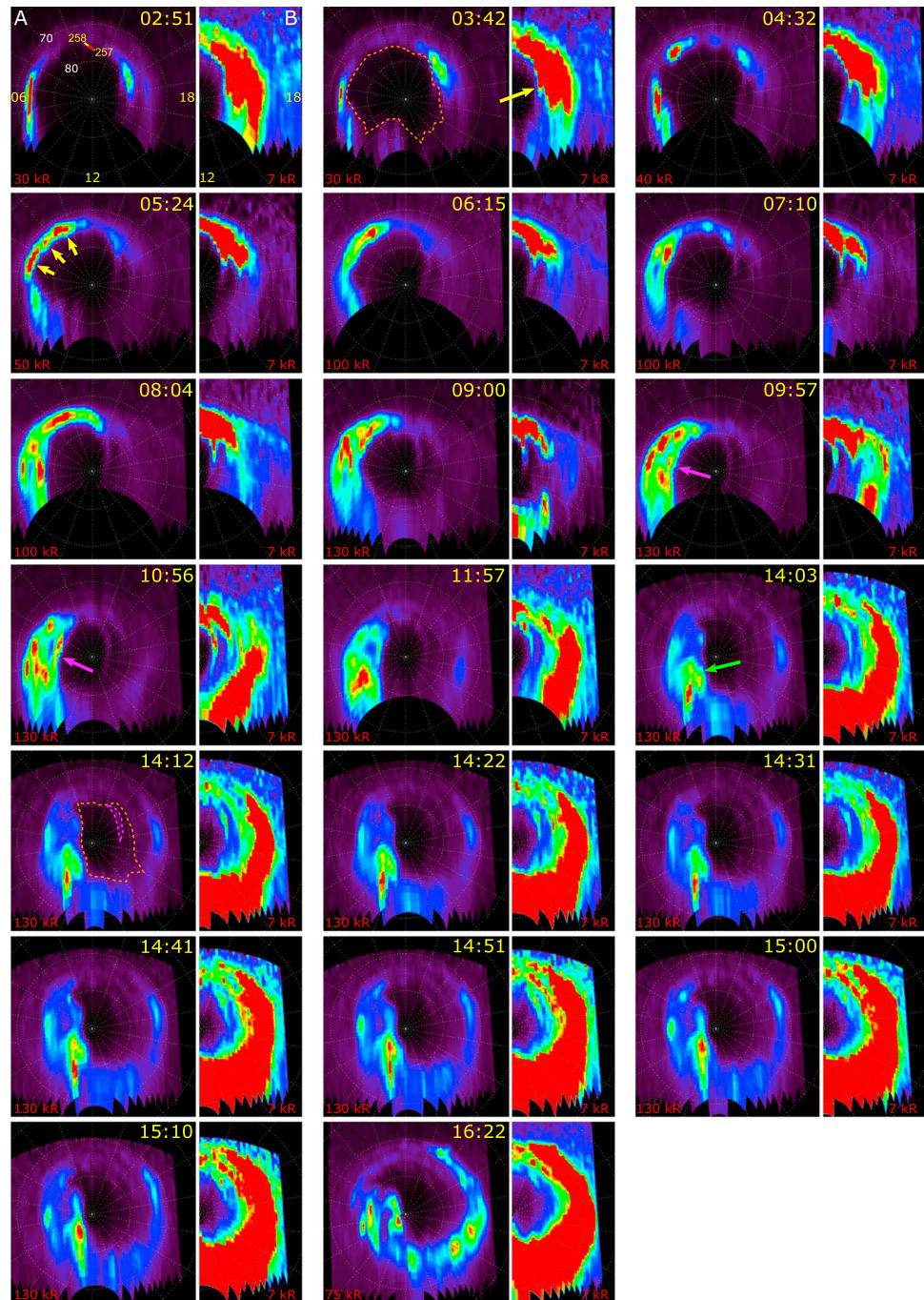


**Figure 1.** Sequence of polar projections of UVIS pseudocolor images of the northern FUV aurora, taken on 14 September 2017 (DOY 257) from 02:51 UT to 17:22 UT (spacecraft time). Each pseudocolor image is reproduced twice: (A) complete polar projection and (B) dusk half (noon to midnight) of the polar projection with saturated color scale. The direction of the Sun (12 LT) is toward the bottom of the images and dusk (18 LT) to the right. The color scale in panels (A) varies along the sequence and the intensity value above which the color scale is saturated is indicated at the bottom of each frame. The start of acquisition time in UT is given on the right upper corner. On the first frame, the magnetically mapped Cassini trajectory during day 257/2017 is drawn in yellow and red, with the red section corresponding to the interval covered by the UVIS sequence. On the panels at 03:42 and 14:12 UT the orange dashed lines give the approximate boundaries of the open magnetic flux region (polar cap), while the pink dashed lines bound the closed flux of the polar arc. The yellow arrow at 03:42 UT points to the protrusion which evolves later as the polar arc described in section 4. At 05:24 UT, three yellow arrows indicate possible signatures of magnetic dipolarization. The pink arrows at 09:57 UT and 10:56 UT show poleward boundary intensifications discussed in section 3. The green arrow at 14:03 UT points to the polar dawn arc described in section 5. UVIS = Ultraviolet Imaging Spectrograph; FUV = far ultraviolet; DOY = day of year.

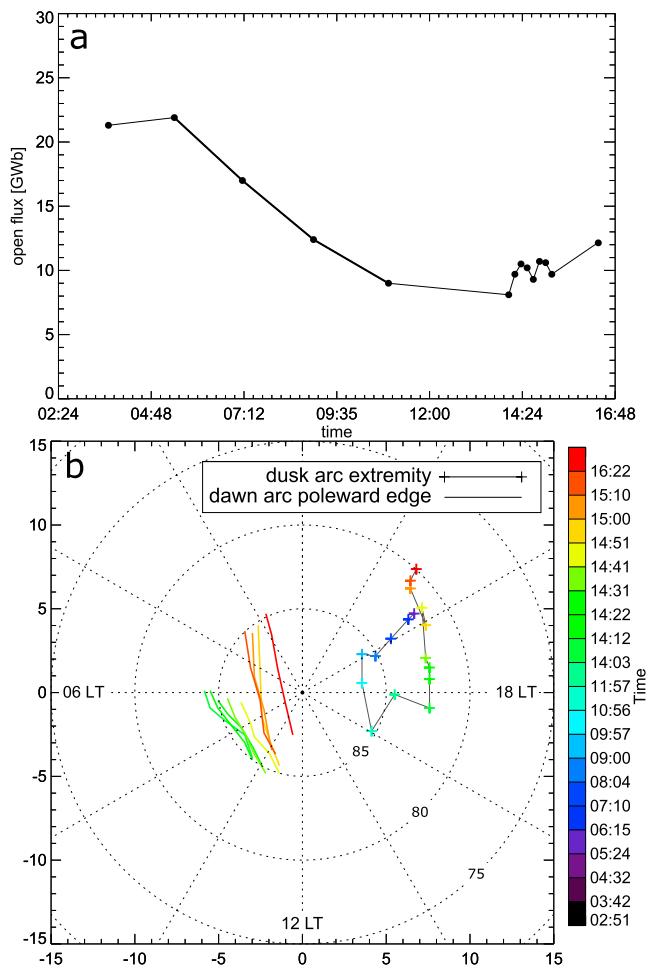


**Figure 2.** (a) Temporal evolution of the open magnetic flux during the UVIS auroral observing sequence shown in Figure 1. Only images where auroral emissions are seen at all longitudes have been included. The method for the determination of the polar cap boundary is described in the text. (b) Polar map showing the displacement of the dayside end of the dusk arc (crosses) from 05:24 to 16:22 UT and the displacement of the poleward edge of the polar dawn arc (lines) from 14:03 to 16:22 UT. The color indicates the start time of each Cassini/UVIS auroral scan. UVIS = Ultraviolet Imaging Spectrograph.

### 3. Auroral Storm

The most striking feature of the UVIS sequence shown in Figure 1 is the broadening of the main emission starting in the midnight-to-dawn sector at 05:24 UT and propagating afterward toward the dayside. During the poleward expansion of the dawn arc of the main emission, its intensity rapidly increases to a peak value of  $\sim 180$  kR at 08:04 UT. This patchy emission remains bright for more than 4 hr, with intensity values locally exceeding 120 kR. The bright feature covers approximately the whole midnight-to-dawn quadrant at 05:24 UT and the local time sector from 06 LT to 09 LT at 11:57 UT, corresponding to a displacement of the center of the region of 4.5-hr LT in  $\sim 6.5$  hr. This corresponds to a mean velocity of  $\sim 31\%$  of rigid corotation.

The poleward expansion of the main aurora in the dawn local time sector tends to contract the dark region enclosed by the main auroral emission. Assuming that the main emission is related to the open-closed field line boundary, this dark region, which is sometimes referred to as the polar cap, is considered to thread open magnetic field lines (Badman et al., 2005; Belenkaya et al., 2008; Bunce et al., 2008). The size of this dark region is then controlled by the balance between magnetic flux opening at the dayside magnetopause and flux closure in the magnetotail and can be used to estimate the open flux contained in the magnetosphere. The polar cap boundary was defined every  $10^\circ$  in longitude by the latitude of the strongest positive brightness gradient along the corresponding meridian, following the method described in Badman et al. (2005, 2014), and by adding to this latitude a poleward shift of  $1.5^\circ$  since the upward field-aligned currents associated with the main emission are lying  $\sim 1\text{--}2^\circ$  equatorward of the open-closed field lines boundary (Belenkaya et al., 2014; Hunt et al., 2014, 2015; Jinks et al., 2014; Talboys et al., 2011). For the longitudes at which this brightness gradient could not be determined, the polar cap boundary was linearly interpolated from the boundary locations at the preceding and following meridians. The open flux contained within the polar cap was then calculated using a flux function as described in detail in Badman et al. (2005).

This procedure could not be applied to the six UVIS images in the sequence for which only a fraction of the main emission is visible and no reliable extrapolation was possible. Two examples of polar cap boundaries are shown in Figure 1, at 03:42 and at 14:12 UT. For the image at 14:12 UT, an auroral arc crossed the polar cap on the duskside. This arc is thought to

be threaded by closed magnetic flux tubes (Radioti et al., 2014), as explained below in section 4. For all the images exhibiting this polar arc, the magnetic flux content of the arc was subtracted from the total magnetic flux enclosed by the main emission. The variation of the estimated open flux during the UVIS sequence is shown in Figure 2a. A clear decrease of the open flux content is observed from 05:24 UT, when the auroral storm started to develop, to 10:56 UT (thick line). It should be noted that the open flux content might be even lower at 11:57 UT, but it cannot be calculated since this image does not cover the whole dayside ionosphere. In the last part of the sequence, the amount of open flux started to increase again.

The morphology of the dawn auroral structure together with the contraction of the polar cap size are the typical characteristics of an auroral storm (e.g., Grodent et al., 2005; Meredith et al., 2014). In situ measurements of the solar wind by Cassini during its approach to Saturn in January 2004 combined with simultaneous HST observations of Saturn's aurorae demonstrated that Kronian auroral storms are the ionospheric response to a large increase in solar wind dynamic pressure and magnetic field strength (Badman et al., 2005; Clarke et al., 2005; Cray et al., 2005; Grodent et al., 2005; Kurth et al., 2005). Theoretical considerations proposed that the resulting compression of the magnetosphere would trigger large-scale Dungey-type reconnection closing a significant part of the open flux in the tail lobes and producing the auroral storm (Cowley et al., 2005).

Auroral dawn storms should not be confused with another type of auroral activity at dawn which has been associated with plasma injections produced by tail reconnection between closed field lines (Vasyliūnas cycle; Lamy et al., 2013; Mitchell et al., 2009; Radioti et al., 2016). Contrary to the auroral storms, the polar cap size does not significantly vary during the latter one. Global magnetohydrodynamic simulations of Saturn's magnetosphere indicate that Dungey-type tail reconnection causes motion of flux tubes filled with hot but tenuous plasma from the tail reconnection sites toward the dayside (Jia et al., 2012). These flux tubes produce stronger effects in the magnetosphere and ionosphere, especially on the dawnside, compared to Vasyliūnas cycle reconnection. In particular, they may generate intense field-aligned currents leading to the observed high auroral intensity values ( $>100$  kR) of the dawn storm.

Prior to the poleward expansion of the dawn auroral arc, at 05:24 UT, three consecutive bright spots, indicated by yellow arrows in Figure 1, appeared in the midnight-to-dawn local time sector. These localized intensifications could be produced by ballooning-like instabilities prior to magnetic dipolarization (Yao, Pu, et al., 2017) and have already been identified in Saturn's aurora before global auroral intensification (Radioti et al., 2016).

Additionally, the dawn storm exhibits some auroral structures similar to those observed during terrestrial sub-storm auroral onsets. In particular, the UVIS pseudoimages at 09:57 UT and 10:56 UT show an intensification of the poleward edge of the storm (pink arrows in Figure 1). Brightening of a similar linear auroral structure has also been identified at Saturn during the compression-induced auroral storm described by Nichols et al. (2014). Poleward boundary intensifications (PBIs) of the auroral oval are common at Earth (e.g., Lyons et al., 1999; Nishimura et al., 2013; Zesta et al., 2000) and are often followed by auroral streamers propagating equatorward from the poleward boundary (e.g., Nishimura et al., 2011; Sergeev et al., 2004). At Saturn, Radioti, Grodent, Yao, et al. (2017) identified a similar auroral streamer. In the present Cassini/UVIS auroral observations, auroral spots equatorward of the PBIs could be streamers but the spatial and temporal resolution are not sufficient to determine their direction of propagation. At Earth, PBIs and subsequent streamers are connected to field-aligned currents induced by fast earthward flows in the plasma sheet (Nishimura et al., 2013; Sergeev et al., 2004). Birn et al. (2004) and Henderson (2009) suggested that these earthward flows are associated with dipolarized field lines and magnetotail reconnection. However, the exact relation between streamers and substorm onset remains an open question (Yao, Pu, et al., 2017). At Saturn, shear-driven field-aligned currents along fast inward flows are expected to produce auroral streamers (Radioti, Grodent, Yao, et al., 2017).

The auroral storm is not limited to its FUV auroral signature. It has also been detected by other Cassini instruments. The top panel of Figure 3 displays observations of auroral radio emissions by the Radio and Plasma Wave Science (RPWS) instrument (Gurnett et al., 2004) at frequencies from 3.5 kHz to 1.6 MHz. This frequency range is dominated by Saturn Kilometric Radiation (SKR, see, e.g., Kaiser et al., 1984; Lamy et al., 2008). The flux density is normalized to 1 AU for comparison purposes with previous SKR studies. The bottom panels of Figure 3 reproduce the magnetic field measurements by Cassini's magnetometer (Dougherty et al., 2004) in spherical radial ( $r$ ), latitudinal ( $\theta$ ), and azimuthal ( $\phi$ ) coordinates referenced to the planet's northern spin axis, after subtraction of the Burton et al.'s (2010) internal field model.

From 07:10 UT on, the magnetic data reveal an increase of the  $B_\theta$  component of the magnetic field coupled with a decrease of the  $B_r$  component, which can be interpreted as a signature of magnetospheric current redistribution, that is, a dipolarization (e.g., Bunce et al., 2005; Jackman et al., 2007, 2008; Yao, Grodent, et al., 2017). Quasi-sinusoidal variability with  $\sim 10.7$ -hr periodicities is also seen in the magnetic field with modulations in the latitudinal component of the field  $\sim 180^\circ$  out of phase with the radial and azimuthal components, consistent with the planetary period oscillations (PPOs) commonly observed in Saturn's magnetosphere (e.g., Andrews et al., 2010; Provan et al., 2018), and in particular in Saturn's magnetic tail (e.g., Cowley & Provan, 2017; Provan et al., 2012; Thomsen et al., 2017). The dipolarization signature observed here is distinguished from PPO signatures due to the fact that while the enhancement of the latitudinal field may be confused with the PPO effects, the decrease in the latitudinal field following the dipolarization signature is not synchronized with the PPO modulations. Furthermore, short time scale fluctuations in all components of the magnetic field immediately after this signature (after  $\sim 09:30$  UT) is consistent with the presence of hot plasma, indicative of the planetward injection of particles accelerated in such a dipolarization.

Additionally, the SKR spectrum exhibits a strong intensification with an extension down to a few kHz from 05:30 to 14:00 UT before the SKR activity gradually returns to a more usual level at the end of the day. The highest SKR intensities at low frequencies are encountered when the UV aurora brightness are also the highest (at 07:10 UT). Such short SKR low-frequency extensions have been shown to be a good proxy for magnetotail

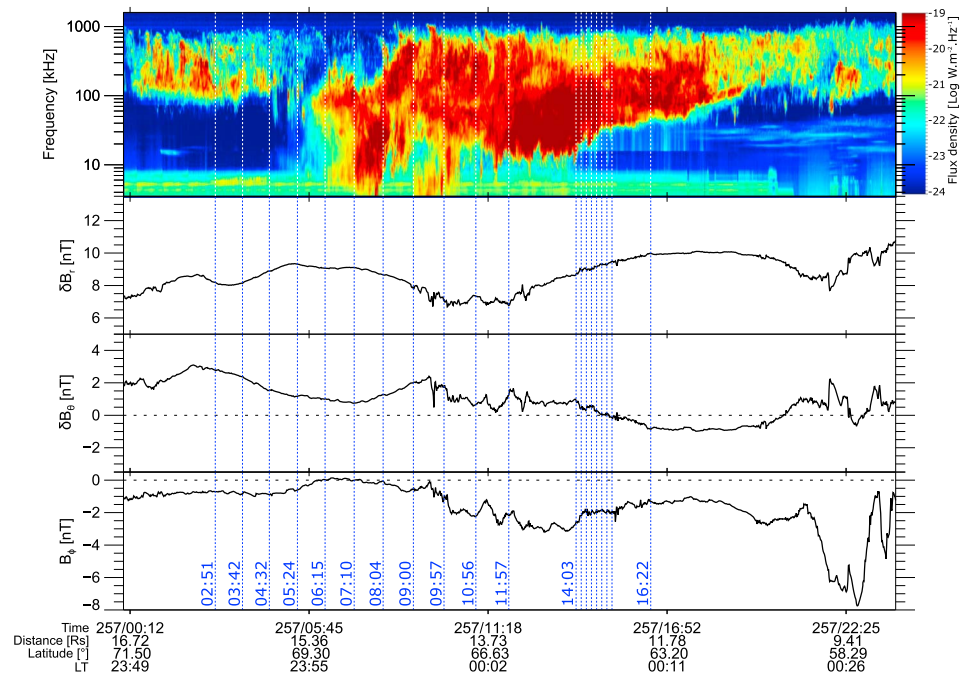


**Figure 3.** Field and plasma measurements on 14 September 2017 (DOY 257). (top panel) Cassini/RPWS frequency-time electric field spectrogram. (bottom panels) Magnetic field components in spherical polar coordinates ( $B_r$ ,  $B_\theta$ , and  $B_\phi$ ) after subtraction of the Burton et al. (2010) internal field model. The vertical dashed lines indicate the start of the acquisition time of UVIS pseudoimages. RPWS = Radio and Plasma Wave Science; UVIS = Ultraviolet Imaging Spectrograph.

reconnection events (Jackman et al., 2009; Reed et al., 2018). The SKR intensity values reached during the storm ( $>10^{-19} \text{ W} \cdot \text{m}^{-2} \cdot \text{Hz}^{-1}$ ) belongs to the 1% most intense events (Lamy et al., 2008). Earlier on the same day, between 03:00 and 05:20 UT, the radial component of the magnetic field increased and peaked strikingly close to the start of the global SKR intensification. This  $B_r$  increase may be indicative of a compression of the magnetosphere which may have triggered the tail reconnection that gave rise to the auroral storm. It is also noteworthy that the three bright auroral spots on the UVIS image starting at 05:24 UT and which could be generated by magnetic dipolarization, appear just after the start time of the SKR enhancement.

Whether the compression of the magnetosphere and the auroral storm are induced by a change in the solar wind conditions cannot be directly assessed. Contrary to the aforementioned simultaneous HST/Cassini observations in January 2004 when the Cassini spacecraft was upstream in the solar wind, during the interval here, Cassini was embedded in the nightside magnetosphere with no possibility to monitor the interplanetary conditions.

Nevertheless, Figure 3 shows a SKR intensification lasting for at least  $\sim 15$  hr (more than a planetary rotation period) before recovering to a more usual level. A 15-hr duration falls below the 20 hr typical limit found by Reed et al. (2018) to discriminate between solar wind-driven ( $>20$  hr) and internally driven ( $<20$  hr) SKR enhancements. However, similarly to long-lasting intensifications triggered by interplanetary shocks (Jackman et al., 2009; Lamy et al., 2013), the SKR enhancement visible in Figure 3 is not in phase with northern regular SKR bursts, the latter being observed between 00 and 05 UT and every  $\sim 10.7$  hr on the days before.

Furthermore, a particle instrument on board Cassini provides another clue supporting a solar wind origin for this event. As explained by Roussos, Jackman, et al. (2018), the high energy of solar energetic particles and galactic cosmic rays (GCRs) allows them to penetrate the magnetosphere and thus to be detected by the Low Energy Magnetospheric Measurement System (LEMMS) of Cassini's Magnetosphere Imaging Instrument (MIMI, Krimigis et al., 2004). Therefore, these particles can be used as tracers of enhanced solar wind conditions such as interplanetary coronal mass ejections (ICMEs). Using the Roussos, Jackman, et al. (2018) method, Roussos, Krupp, et al. (2018) identified the onset of a particularly energetic ICME event on day 255 of 2017. On day 257, during UVIS auroral imaging, a sharp increase in the flux of energetic protons was observed, which

might correspond to the arrival of the associated interplanetary shock. Due to the end of the mission on the following day, the exact time of arrival of the interplanetary shock cannot be assessed in this case. Nevertheless, these observations suggest that the compression of the magnetosphere observed in the magnetic field data that may induce the auroral storm was caused by the upcoming arrival of a strong ICME shock at Saturn. Furthermore, this energetic ICME could be the counterpart of a powerful solar flare, which was expelled from the Sun 8 days before the current auroral observations (Roussos, Krupp, et al., 2018).

Finally, this interpretation of plasma data is also consistent with solar wind parameters propagated from the Earth to Saturn discussed in Lamy et al. (2018). Despite their large uncertainty, both models indicate the arrival of an interplanetary shock close to day 257/2017. These three different methods to infer the solar wind conditions at Saturn during the UVIS observing time are then in good agreement, and we can conclude that the UV auroral storm and the SKR intensification most likely result from an ICME shock.

#### 4. Nightside Auroral Arc Across the Polar Cap

The dawn auroral storm being very bright, faint auroral structures on the duskside are apparent only after saturation of the color scale to low values of intensity. The noon-to-midnight sector via dusk of the saturated projection is given for each pseudoimage on the right panels (B) in Figure 1. At 03:42 UT, a protrusion, indicated by a yellow arrow, grows away from the main postdusk auroral arc. The protrusion evolves little for the next 3.5 hr before starting to move poleward and to extend toward the dayside. This arc stays attached to the nightside main emission and extends through the polar region, which is generally devoid of emission. Figure 2b highlights the motion of the arc by showing the evolution of the position of its dayside end (colored crosses), determined by an intensity drop below 3 kR. The maximal extension of this polar arc is reached at 10:56 UT when it extends over more than 120° of longitude and is almost connected to the dayside main auroral emissions. At the same time, other arcs are seen at lower latitudes in the postdusk sector. Later in the auroral sequence, the polar arc moves equatorward until 14:03 UT when it starts to shorten (see Figure 2b). On the three last images, the polar arc appears only as a small spot.

This polar arc observed on the duskside of the magnetosphere is morphologically similar to nightside polar arcs commonly observed at Earth (e.g., Carter et al., 2017; Fear et al., 2014; Kullen et al., 2002; Milan et al., 2005; Zhu et al., 1997). These auroral structures can come off a side of the auroral oval or protrude from the nightside oval through the polar cap and occasionally reach the dayside of the auroral oval (Kullen et al., 2002). At Saturn, a similar nightside arc was identified by Radioti et al. (2014). Interestingly, their observation of such an arc was concurrent with an auroral storm on the dawnside although the authors argued that the two events were independent. At the start of their observations, the arc was already formed and was still present about 3 hr later at the end of the observation time. Although they did not have observational evidence of the formation of this elusive arc, they suggested that it formed during a period of enhanced Dungey-type tail reconnection and in the absence of dayside reconnection (under southward IMF conditions), similarly to the mechanism described by Milan et al. (2005) and Fear and Milan (2012) for the terrestrial nightside polar arcs. In addition, the rotation-driven tail reconnection on closed field lines (Vasyliūnas type) should be suppressed. This scenario implies that the arc protruded from the nightside of the main emission. The long UVIS sequence presented in the current paper is the first study to validate this scenario.

We suggest that at the start of the sequence, southward IMF conditions prevent the opening of flux at the nose of the magnetosphere. From 07:10 UT onward, a buildup of closed flux tubes embedded within the polar cap caused by enhanced Dungey tail reconnection leads to the elongation of the nightside arc toward the dayside. Tail reconnection is also responsible for the auroral dawn storm and, combined with the absence of dayside reconnection, for the contraction of the polar cap discussed in section 3. Simultaneously, high-latitude reconnection in the lobe redistributes open flux in the polar cap, causing a dawnward motion of the extending arc, as we observe at Earth (Fear et al., 2014, 2015; Milan et al., 2005). From 09:57 UT onward, an equatorward motion of the arc is noted, indicating a change in the IMF  $B_y$  component. At 11:57 UT, the dawn storm starts to vanish, the polar cap ceases to contract, and the polar arc starts to shorten, suggesting less active magnetotail reconnection. This also implies the initiation of low-latitude dayside reconnection that opens flux at the magnetopause and releases the closed flux of the polar arc. This is only possible after a reversal of the IMF from southward to northward. The end of the high-latitude lobe reconnection due to the IMF reversal stops

the equatorward displacement of the arc. Unfortunately, we do not have concurrent measurements of the interplanetary magnetic field to infer its orientation and to validate our scenario.

### 5. High-Latitude Dawn Polar Arc

At the end of the auroral storm, an arc-like structure, indicated by a green arrow at 14:03 UT in Figure 1 starts to develop in the dawn-to-noon sector. Due to a  $\sim 2$ -hr gap in the UVIS observations before the pseudoimage at 14:03 UT, it is difficult to determine if this arc appears postdawn or if it is a remnant of the storm. Later, the higher temporal resolution of the observations enables us to easily track the evolution of the arc. The position of its poleward edge from 14:03 UT to the end of the sequence is shown by the color-coded lines in Figure 2b. This dawn arc moves toward the pole and seems to extend toward the nightside. On the final image, the arc is located at a colatitude of only  $1.2^\circ$ , making it one of the most polar auroral structures ever observed at Saturn.

Auroral emissions at dawn close to the poles have been observed on 26 and 28 January 2004 during the HST campaign simultaneous to the Cassini approach (Clarke et al., 2005; Grodent et al., 2005). In these previous observations, the polar dawn emission was associated with the arrival of a solar wind pressure pulse and was filled with flux tubes recently closed in the tail (Cowley et al., 2005). An HST image of Saturn's aurora on 13 February 2008 showed a similar structure but the observation geometry made it difficult to precisely know its morphology (Clarke et al., 2009). Nevertheless, Clarke et al. (2009) suggested that it might be interpreted as a dawn storm, similar to that observed in 2004.

In our observations, we cannot exclude that the polar dawn arc is a remnant of the vanishing auroral storm. However, this feature might also be independent from the storm and could be produced by dayside reconnection at the magnetopause. The occurrence of magnetopause reconnection is suggested by the shortening of the nightside polar arc at dusk (section 4) and by the increase of the open flux contained in the magnetosphere (Figure 2a). In both cases, the poleward motion might result from magnetic field reconfiguration and current redistribution induced by the magnetospheric compression subsequent to the crossing of the ICME shock, whose onset triggered the auroral storm a few hours earlier. Such poleward motion of auroral structures due to current redistribution in the magnetosphere has already been observed at Saturn (Radioti, Grodent, Yao, et al., 2017) and has been modeled for the Earth's magnetosphere (Chu et al., 2015).

### 6. Summary

In the present study, we describe the final Cassini/UVIS observations of Saturn's FUV northern auroral emissions. This observation sequence allows us to follow the evolution of auroral structures over 14 hr. In particular, an auroral storm developed on the dawnside and was followed by one of the most polar auroral structures observed at Saturn. Simultaneously, the evolution of a nightside polar arc at dusk was tracked for the first time from its growth until the end of its decay, showing evidence of its formation process. From these observations, we could propose a scenario of the dynamics occurring in Saturn's magnetosphere over this period.

At the start of day 257/2017, Saturn's magnetosphere was compressed, as suggested in magnetic field measurements, likely due to the onset of a strong ICME event. We argue that this solar wind-induced compression enhanced Dungey-type magnetotail reconnection resulting in the growth of an UV auroral storm in the dawnside ionosphere from  $\sim 05:30$  UT and, due to the absence of dayside magnetopause reconnection under southward IMF conditions, in a decrease of the open flux content in the magnetosphere. Perturbations in the magnetic field are compatible with magnetic dipolarization associated with the tail reconnection. Simultaneously, a very strong intensification of SKR and its extension to lower frequencies are additional sign of the solar wind-induced magnetotail reconnection. We suggest that the absence of dayside reconnection leads to a buildup of closed flux into the open field line polar cap region, forming a polar arc at dusk extending to the dayside. High-latitude lobe reconnection induces a poleward motion of this polar arc from  $\sim 07$  until  $\sim 10$  UT when a change in the IMF  $B_y$  component occurred as shown by the equatorward motion of the arc from this time on.

At  $\sim 12$  UT, magnetotail reconnection rate had decreased, the polar cap ceased contracting, and the polar arc at dusk had reached its maximal extension. Two hours later, a reversal of the IMF  $B_z$  to northward allowed the initiation of low-latitude magnetopause reconnection, as shown by a slight increase of the open flux content and the reduction of closed flux tubes forming the polar nightside arc at dusk. The atypical prenoon arc

moving poleward up to very high latitudes might be a signature of magnetopause reconnection, and its poleward motion can be caused by the arrival at Saturn of the ICME shock.

The ultimate Cassini/UVIS auroral observations have once again demonstrated the importance of auroral imaging for the understanding of the dynamics in planetary magnetospheres.

#### Acknowledgments

B. P., D. G., and J. C. G. are supported by the PRODEX program managed by ESA in collaboration with the Belgian Federal Science Policy Office. Z. H. Y. is funded by a Marie Curie COFUND postdoctoral fellowship. T. J. B. is supported by STFC Quota Studentship ST/N504117/1. L. L. is supported by CNES and CNRS/INSU programs of heliophysics and planetology. E. J. B. and S. W. H. C. are supported by STFC Consolidated grant ST/N000749/1. E. J. B. is supported by a Royal Society Wolfson Research Merit Award. The research at the University of Iowa was supported by NASA through contract 1415150 with the Jet Propulsion Laboratory. W. R. P. acknowledges support from the NASA JPL Cassini Project. B. P. would like to acknowledge Steve Milan and Robert Fear for helpful explanations about the motion of transpolar auroral arcs at Earth. The Cassini/UVIS, MAG and RPWS data used in this study will be soon available through the Planetary Data System (<https://pds.nasa.gov>).

#### References

- Andrews, D. J., Cowley, S. W. H., Dougherty, M. K., & Provan, G. (2010). Magnetic field oscillations near the planetary period in Saturn's equatorial magnetosphere: Variation of amplitude and phase with radial distance and local time. *Journal of Geophysical Research*, *115*, A04212. <https://doi.org/10.1029/2009JA014729>
- Badman, S. V., Branduardi-Raymont, G., Galand, M., Hess, S. L. G., Krupp, N., Lamy, L., et al. (2015). Auroral processes at the giant planets: Energy deposition, emission mechanisms, morphology and spectra. *Space Science Reviews*, *187*, 99–179. <https://doi.org/10.1007/s11214-014-0042-x>
- Badman, S. V., Bunce, E. J., Clarke, J. T., Cowley, S. W. H., Gérard, J.-C., Grodent, D., & Milan, S. E. (2005). Open flux estimates in Saturn's magnetosphere during the January 2004 Cassini-HST campaign, and implications for reconnection rates. *Journal of Geophysical Research*, *110*, A11216. <https://doi.org/10.1029/2005JA011240>
- Badman, S. V., & Cowley, S. W. H. (2007). Significance of Dungey-cycle flows in Jupiter's and Saturn's magnetospheres, and their identification on closed equatorial field lines. *Annales Geophysicae*, *25*, 941–951. <https://doi.org/10.5194/angeo-25-941-2007>
- Badman, S. V., Jackman, C. M., Nichols, J. D., Clarke, J. T., & Gérard, J.-C. (2014). Open flux in Saturn's magnetosphere. *Icarus*, *231*, 137–145. <https://doi.org/10.1016/j.icarus.2013.12.004>
- Belenkaya, E. S., Cowley, S. W. H., Badman, S. V., Blokhina, M. S., & Kalegaev, V. (2008). Dependence of the open-closed field line boundary in Saturn's ionosphere on both the IMF and solar wind dynamic pressure: Comparison with the UV auroral oval observed by the HST. *Annales Geophysicae*, *26*, 159–166. <https://doi.org/10.5194/angeo-26-159-2008>
- Belenkaya, E. S., Cowley, S. W. H., Meredith, C. J., Nichols, J. D., Kalegaev, V. V., Alexeev, I. I., et al. (2014). Magnetospheric magnetic field modelling for the 2011 and 2012 HST Saturn aurora campaigns—Implications for auroral source regions. *Annales Geophysicae*, *32*, 689–704. <https://doi.org/10.5194/angeo-32-689-2014>
- Birn, J., Raeder, J., Wang, Y. L., Wolf, R. A., & Hesse, M. (2004). On the propagation of bubbles in the geomagnetic tail. *Annales Geophysicae*, *22*, 1773–1786. <https://doi.org/10.5194/angeo-22-1773-2004>
- Blanc, M., Andrews, D. J., Coates, A. J., Hamilton, D. C., Jackman, C. M., Jia, X., et al. (2015). Saturn plasma sources and associated transport processes. *Space Science Reviews*, *192*, 237–283. <https://doi.org/10.1007/s11214-015-0172-9>
- Broadfoot, A. L., Sandel, B. R., Shemansky, D. E., Holberg, J. B., Smith, G. R., Strobel, D. F., et al. (1981). Extreme ultraviolet observations from Voyager 1 encounter with Saturn. *Science*, *212*(4491), 206–211. <https://doi.org/10.1126/science.212.4491.206>
- Bunce, E. J., Arridge, C. S., Clarke, J. T., Clarke, J. T., Coates, A. J., Cowley, S. W. H., et al. (2008). Origin of Saturn's aurora: Simultaneous observations by Cassini and the Hubble Space Telescope. *Journal of Geophysical Research*, *113*, A09209. <https://doi.org/10.1029/2008JA013257>
- Bunce, E. J., Cowley, S. W. H., Alexeev, I. I., Arridge, C. S., Dougherty, M. K., Nichols, J. D., & Russell, C. T. (2007). Cassini observations of the variation of Saturn's ring current parameters with system size. *Journal of Geophysical Research*, *112*, A10202. <https://doi.org/10.1029/2007JA012275>
- Bunce, E. J., Cowley, S. W. H., Wright, D. M., Coates, A. J., Dougherty, M. K., Krupp, N., et al. (2005). In situ observations of a solar wind compression-induced hot plasma injection in Saturn's tail. *Geophysical Research Letters*, *32*, L20504. <https://doi.org/10.1029/2005GL022888>
- Burton, M. E., Dougherty, M. K., & Russell, C. T. (2010). Saturn's internal planetary magnetic field. *Geophysical Research Letters*, *37*, L24105. <https://doi.org/10.1029/2010gl045148>
- Carter, J. A., Milan, S. E., Fear, R. C., Walach, M.-T., Harrison, Z. A., Paxton, L. J., & Hubert, B. (2017). Transpolar arcs observed simultaneously in both hemispheres. *Journal of Geophysical Research: Space Physics*, *122*, 6107–6120. <https://doi.org/10.1002/2016JA023830>
- Chu, X., McPherron, R. L., Hsu, T.-S., Angelopoulos, V., Pu, Z., Yao, Z., et al. (2015). Magnetic mapping effects of substorm currents leading to auroral poleward expansion and equatorward retreat. *Journal of Geophysical Research: Space Physics*, *120*, 253–265. <https://doi.org/10.1002/2014JA020596>
- Clarke, J. T., Gérard, J.-C., Grodent, D., Wannawichian, S., Gustin, J., Connerney, J., et al. (2005). Morphological differences between Saturn's ultraviolet aurorae and those of Earth and Jupiter. *Nature*, *433*(7027), 717–719. <https://doi.org/10.1038/nature03331>
- Clarke, J. T., Moos, H. W., Atreya, S. K., & Lane, A. L. (1981). IUE detection of bursts of H Ly $\alpha$  emission from Saturn. *Nature*, *290*(5803), 226–227. <https://doi.org/10.1038/290226a0>
- Clarke, J. T., Nichols, J., Gérard, J.-C., Grodent, D., Hansen, K. C., Kurth, W., et al. (2009). Response of Jupiter's and Saturn's auroral activity to the solar wind. *Journal of Geophysical Research*, *114*, A05210. <https://doi.org/10.1029/2008JA013694>
- Cowley, S. W. H., Badman, S. V., Bunce, E. J., Clarke, J. T., Gérard, J.-C., Grodent, D., et al. (2005). Reconnection in a rotation-dominated magnetosphere and its relation to Saturn's auroral dynamics. *Journal of Geophysical Research*, *110*, A02201. <https://doi.org/10.1029/2004JA010796>
- Cowley, S. W. H., & Provan, G. (2017). Planetary period modulations of Saturn's magnetotail current sheet during northern spring: Observations and modeling. *Journal of Geophysical Research: Space Physics*, *122*, 6049–6077. <https://doi.org/10.1002/2017JA023993>
- Crary, F. J., Clarke, J. T., Dougherty, M. K., Hanlon, P. G., Hansen, K. C., Steinberg, J. T., et al. (2005). Solar wind dynamic pressure and electric field as the main factors controlling Saturn's aurorae. *Nature*, *433*, 720–722. <https://doi.org/10.1038/nature03333>
- Dougherty, M. K., Kellock, S., Southwood, D. J., Balogh, A., Smith, E. J., Tsurutani, B. T., et al. (2004). The Cassini magnetic field investigation. *Space Science Review*, *114*, 331–383. <https://doi.org/10.1007/s11214-004-1432-2>
- Dungey, J. W. (1961). Interplanetary magnetic field and the auroral zones. *Physical Review Letters*, *6*(2), 47–48. <https://doi.org/10.1103/physrevlett.6.47>
- Esposito, L. W., Barth, C. A., Colwell, J. E., Lawrence, G. M., McClintock, W. E., Stewart, A. I. F., et al. (2004). The Cassini ultraviolet imaging spectrograph investigation. *Space Science Review*, *115*, 299–361. <https://doi.org/10.1007/s11214-004-1455-8>
- Fear, R. C., & Milan, S. E. (2012). The IMF dependence of the local time of transpolar arcs: Implications for formation mechanism. *Journal of Geophysical Research*, *117*, A03213. <https://doi.org/10.1029/2011JA017209>
- Fear, R. C., Milan, S. E., Carter, J. A., & Maggiolo, R. (2015). The interaction between transpolar arcs and cusp spots. *Geophysical Research Letters*, *42*, 9685–9693. <https://doi.org/10.1002/2015GL066194>

- Fear, R. C., Milan, S. E., Maggiolo, R., Fazakerley, A. N., Dandouras, I., & Mende, S. B. (2014). Direct observation of closed magnetic flux trapped in the high-latitude magnetosphere. *Science*, *346*(6216), 1506–1510. <https://doi.org/10.1126/science.1257377>
- Gérard, J.-C., Bonfond, B., Gustin, J., Grodent, D., Clarke, J. T., Bisikalo, D., & Schematovich, V. (2009). Altitude of Saturn's aurora and its implications for the characteristic energy of precipitated electrons. *Geophysical Research Letters*, *36*, L02202. <https://doi.org/10.1029/2008GL036554>
- Gérard, J. C., Dols, V., Grodent, D., Waite, J. H., Gladstone, G. R., & Prangé, R. (1995). Simultaneous observations of the Saturnian aurora and polar haze with the HST/FOC. *Geophysical Research Letters*, *22*(20), 2685–2688. <https://doi.org/10.1029/95GL02645>
- Gérard, J.-C., Grodent, D., Gustin, J., Saglam, A., Clarke, J. T., & Trauger, J. T. (2004). Characteristics of Saturn's FUV aurora observed with the Space Telescope Imaging Spectrograph. *Journal of Geophysical Research*, *109*, A09207. <https://doi.org/10.1029/2004JA010513>
- Grodent, D. (2015). A brief review of ultraviolet auroral emissions on giant planets. *Space Science Reviews*, *187*(1), 23–50. <https://doi.org/10.1007/s11214-014-0052-8>
- Grodent, D., Gérard, J.-C., Cowley, S. W. H., Bunce, E. J., & Clarke, J. T. (2005). Variable morphology of Saturn's southern ultraviolet aurora. *Journal of Geophysical Research*, *110*, A07215. <https://doi.org/10.1029/2004JA010983>
- Grodent, D., Gustin, J., Gérard, J.-C., Radioti, A., Bonfond, B., & Pryor, W. R. (2011). Small-scale structures in Saturn's ultraviolet aurora. *Journal of Geophysical Research*, *116*, A09225. <https://doi.org/10.1029/2011JA016818>
- Gurnett, D. A., Kurth, W. S., Kirchner, D. L., Hospodarsky, G. B., Averkamp, T. F., Zarka, P., et al. (2004). The Cassini radio and plasma wave investigation. *Space Science Review*, *114*, 395–463. <https://doi.org/10.1007/s11214-004-1434-0>
- Gustin, J., Grodent, D., Radioti, A., Pryor, W., Lamy, L., & Ajello, J. (2017). Statistical study of Saturn's auroral electron properties with Cassini/UVIS FUV spectral images. *Icarus*, *284*, 264–283. <https://doi.org/10.1016/j.icarus.2016.11.017>
- Henderson, M. G. (2009). Observational evidence for an inside-out substorm onset scenario. *Annales Geophysicae*, *27*, 2129–2140. <https://doi.org/10.5194/angeo-27-2129-2009>
- Hunt, G. J., Cowley, S. W. H., Provan, G., Bunce, E. J., Alexeev, I. I., Belenkaya, E. S., et al. (2014). Field-aligned currents in Saturn's southern nightside magnetosphere: Subcorotation and planetary period oscillation components. *Journal of Geophysical Research: Space Physics*, *119*, 9847–9899. <https://doi.org/10.1002/2014JA020506>
- Hunt, G. J., Cowley, S. W. H., Provan, G., Bunce, E. J., Alexeev, I. I., Belenkaya, E. S., et al. (2015). Field-aligned currents in Saturn's northern nightside magnetosphere: Evidence for interhemispheric current flow associated with planetary period oscillations. *Journal of Geophysical Research: Space Physics*, *120*, 7552–7584. <https://doi.org/10.1002/2015JA021454>
- Jackman, C. M., Arridge, C. S., Krupp, N., Bunce, E. J., Mitchell, D. G., McAndrews, H. J., et al. (2008). A multi-instrument view of tail reconnection at Saturn. *Journal of Geophysical Research*, *113*, A11213. <https://doi.org/10.1029/2008JA013592>
- Jackman, C. M., Lamy, L., Freeman, M. P., Zarka, P., Cecconi, B., Kurth, W. S., et al. (2009). On the character and distribution of lower-frequency radio emissions at Saturn and their relationship to substorm-like events. *Journal of Geophysical Research*, *114*, A08211. <https://doi.org/10.1029/2008JA013997>
- Jackman, C. M., Russell, C. T., Southwood, D. J., Arridge, C. S., Achilleos, N., & Dougherty, M. K. (2007). Strong rapid dipolarizations in Saturn's magnetotail: In situ evidence of reconnection. *Geophysical Research Letters*, *34*, L11203. <https://doi.org/10.1029/2007GL029764>
- Jackman, C. M., Slavin, J. A., & Cowley, S. W. H. (2011). Cassini observations of plasmoid structure and dynamics: Implications for the role of magnetic reconnection in magnetospheric circulation at Saturn. *Journal of Geophysical Research*, *116*, A10212. <https://doi.org/10.1029/2011JA016682>
- Jia, X., Hansen, K. C., Gombosi, T. I., Kivelson, M. G., Tóth, G., DeZeeuw, D. L., & Ridley, A. J. (2012). Magnetospheric configuration and dynamics of Saturn's magnetosphere: A global MHD simulation. *Journal of Geophysical Research*, *117*, A05225. <https://doi.org/10.1029/2012JA017575>
- Jinks, S. L., Bunce, E. J., Cowley, S. W. H., Provan, G., Yeoman, T. K., Arridge, C. S., et al. (2014). Cassini multi-instrument assessment of Saturn's polar cap boundary. *Journal of Geophysical Research: Space Physics*, *119*, 8161–8177. <https://doi.org/10.1002/2014JA020367>
- Judge, D. L., Wu, F. M., & Carlson, R. W. (1980). Ultraviolet photometer observations of the Saturnian system. *Science*, *207*(4429), 431–434. <https://doi.org/10.1126/science.207.4429.431>
- Kaiser, M. L., Desch, M. D., Kurth, W. S., Lecacheux, A., Genova, F., Pedersen, B. M., & Evans, D. R. (1984). Saturn. chap. Saturn as a radio source, pp. 378–415.
- Krimigis, S. M., Mitchell, D. G., Hamilton, D. C., Livi, S., Dandouras, J., Jaskulek, S., et al. (2004). Magnetosphere Imaging Instrument (MIMI) on the Cassini mission to Saturn/Titan. *Space Science Review*, *114*, 233–329. <https://doi.org/10.1007/s11214-004-1410-8>
- Kullen, A., Brittnacher, M., Cumnock, J. A., & Blomberg, L. G. (2002). Solar wind dependence of the occurrence and motion of polar auroral arcs: A statistical study. *Journal of Geophysical Research*, *107*(A11), 1362. <https://doi.org/10.1029/2002JA009245>
- Kurth, W. S., Gurnett, D. A., Clarke, J. T., Zarka, P., Desch, M. D., Kaiser, M. L., et al. (2005). An Earth-like correspondence between Saturn's auroral features and radio emission. *Nature*, *433*, 722–725. <https://doi.org/10.1038/nature03334>
- Lamy, L., Prangé, R., Pryor, W., Gustin, J., Badman, S. V., Melin, H., et al. (2013). Multispectral simultaneous diagnosis of Saturn's aurorae throughout a planetary rotation. *Journal of Geophysical Research: Space Physics*, *118*, 4817–4843. <https://doi.org/10.1002/jgra.50404>
- Lamy, L., Prangé, R., Tao, C., Kim, T., Badman, S. V., Zarka, P., et al. (2018). Saturn's northern aurorae at solstice from HST observations coordinated with Cassini's Grand Finale. *Geophysical Research Letters*, *45*. <https://doi.org/10.1029/2018GL078211>
- Lamy, L., Zarka, P., Cecconi, B., Prangé, R., Kurth, W. S., & Gurnett, D. A. (2008). Saturn kilometric radiation: Average and statistical properties. *Journal of Geophysical Research*, *113*, A07201. <https://doi.org/10.1029/2007JA012900>
- Lyons, L. R., Nagai, T., Blanchard, G. T., Samson, J. C., Yamamoto, T., Mukai, T., et al. (1999). Association between Geotail plasma flows and auroral poleward boundary intensifications observed by CANOPUS photometers. *Journal of Geophysical Research*, *104*(A3), 4485–4500. <https://doi.org/10.1029/1998JA900140>
- McGrath, M. A., & Clarke, J. T. (1992). H I Lyman alpha emission from Saturn (1980–1990). *Journal of Geophysical Research*, *97*(A9), 13,691–13,703. <https://doi.org/10.1029/92JA00143>
- Meredith, C. J., Cowley, S. W. H., & Nichols, J. D. (2014). Survey of Saturn auroral storms observed by the Hubble Space Telescope: Implications for storm time scales. *Journal of Geophysical Research: Space Physics*, *119*, 9624–9642. <https://doi.org/10.1002/2014JA020601>
- Milan, S. E., Hubert, B., & Grocott, A. (2005). Formation and motion of a transpolar arc in response to dayside and nightside reconnection. *Journal of Geophysical Research*, *110*, A01212. <https://doi.org/10.1029/2004JA010835>
- Mitchell, D., Krimigis, S., Paranicas, C., Brandt, P., Carbarary, J., Roelof, E., et al. (2009). Recurrent energization of plasma in the midnight-to-dawn quadrant of Saturn's magnetosphere, and its relationship to auroral UV and radio emissions. *Planetary and Space Science*, *57*, 1732–1742. <https://doi.org/10.1016/j.pss.2009.04.002>
- Nichols, J. D., Badman, S. V., Baines, K. H., Brown, R. H., Bunce, E. J., Clarke, J. T., et al. (2014). Dynamic auroral storms on Saturn as observed by the Hubble Space Telescope. *Geophysical Research Letters*, *41*, 3323–3330. <https://doi.org/10.1002/2014GL060186>

- Nishimura, Y., Lyons, L. R., Angelopoulos, V., Kikuchi, T., Zou, S., & Mende, S. B. (2011). Relations between multiple auroral streamers, pre-onset thin arc formation, and substorm auroral onset. *Journal of Geophysical Research*, *116*, A09214. <https://doi.org/10.1029/2011JA016768>
- Nishimura, Y., Lyons, L. R., Xing, X., Angelopoulos, V., Donovan, E. F., Mende, S. B., et al. (2013). Tail reconnection region versus auroral activity inferred from conjugate ARTEMIS plasma sheet flow and auroral observations. *Journal of Geophysical Research: Space Physics*, *118*, 5758–5766. <https://doi.org/10.1002/jgra.50549>
- Prangé, R., Pallier, L., Hansen, K. C., Howard, R., Vourlidis, A., Courtin, R., & Parkinson, C. (2004). An interplanetary shock traced by planetary auroral storms from the Sun to Saturn. *Nature*, *432*, 78–81. <https://doi.org/10.1038/nature02986>
- Provan, G., Andrews, D. J., Arridge, C. S., Coates, A. J., Cowley, S. W. H., Cox, G., et al. (2012). Dual periodicities in planetary-period magnetic field oscillations in Saturn's tail. *Journal of Geophysical Research*, *117*, A01209. <https://doi.org/10.1029/2011JA017104>
- Provan, G., Cowley, S. W. H., Bradley, T. J., Bunce, E. J., Hunt, G. J., & Dougherty, M. K. (2018). Planetary period oscillations in Saturn's magnetosphere: Cassini magnetic field observations over the northern summer solstice interval. *Journal of Geophysical Research: Space Physics*, *123*, 3859–3899. <https://doi.org/10.1029/2018JA025237>
- Radioti, A., Grodent, D., Gérard, J.-C., Milan, S. E., Fear, R. C., Jackman, C. M., et al. (2014). Saturn's elusive nightside polar arc. *Geophysical Research Letters*, *41*, 6321–6328. <https://doi.org/10.1002/2014GL061081>
- Radioti, A., Grodent, D., Gérard, J.-C., Southwood, D. J., Chané, E., Bonfond, B., & Pryor, W. (2017). Stagnation of Saturn's auroral emission at noon. *Journal of Geophysical Research: Space Physics*, *122*, 6078–6087. <https://doi.org/10.1002/2016JA023820>
- Radioti, A., Grodent, D., Jia, X., Gérard, J.-C., Bonfond, B., Pryor, W., et al. (2016). A multi-scale magnetotail reconnection event at Saturn and associated flows: Cassini/UVIS observations. *Icarus*, *263*, 75–82. <https://doi.org/10.1016/j.icarus.2014.12.016>
- Radioti, A., Grodent, D., Yao, Z. H., Gérard, J.-C., Badman, S. V., Pryor, W., & Bonfond, B. (2017). Dawn auroral breakup at Saturn initiated by auroral arcs: UVIS/Cassini beginning of Grand Finale phase. *Journal of Geophysical Research: Space Physics*, *122*, 12,111–12,119. <https://doi.org/10.1002/2017JA024653>
- Reed, J. J., Jackman, C. M., Lamy, L., Kurth, W. S., & Whiter, D. K. (2018). Low-frequency extensions of the Saturn kilometric radiation as a proxy for magnetospheric dynamics. *Journal of Geophysical Research: Space Physics*, *123*, 443–463. <https://doi.org/10.1002/2017JA024499>
- Roussos, E., Jackman, C. M., Thomsen, M. F., Kurth, W. S., Badman, S. V., Paranicas, C., et al. (2018). Solar Energetic Particles (SEP) and Galactic Cosmic Rays (GCR) as tracers of solar wind conditions near Saturn: Event lists and applications. *Icarus*, *300*, 47–71. <https://doi.org/10.1016/j.icarus.2017.08.040>
- Roussos, E., Krupp, N., Paranicas, C., Kollmann, P., Mitchell, D. G., Krimigis, S. M., & Palmaerts, B. (2018). Heliospheric conditions at Saturn during Cassini's ring-grazing and proximal orbits. *Geophysical Research Letters*, *45*. <https://doi.org/10.1029/2018GL078093>
- Sandel, B. R., & Broadfoot, A. L. (1981). Morphology of Saturn's aurora. *Nature*, *292*(5825), 679–682. <https://doi.org/10.1038/292679a0>
- Sergeev, V. A., Liou, K., Newell, P. T., Ohtani, S.-I., Hairston, M. R., & Rich, F. (2004). Auroral streamers: Characteristics of associated precipitation, convection and field-aligned currents. *Annales Geophysicae*, *22*, 537–548. <https://doi.org/10.5194/angeo-22-537-2004>
- Southwood, D. J., & Chané, E. (2016). High-latitude circulation in giant planet magnetospheres. *Journal of Geophysical Research: Space Physics*, *121*, 5394–5403. <https://doi.org/10.1002/2015JA022310>
- Talboys, D. L., Bunce, E. J., Cowley, S. W. H., Arridge, C. S., Coates, A. J., & Dougherty, M. K. (2011). Statistical characteristics of field-aligned currents in Saturn's nightside magnetosphere. *Journal of Geophysical Research*, *116*, A04213. <https://doi.org/10.1029/2010JA016102>
- Thomsen, M. F., Jackman, C. M., Cowley, S. W. H., Jia, X., Kivelson, M. G., & Provan, G. (2017). Evidence for periodic variations in the thickness of Saturn's nightside plasma sheet. *Journal of Geophysical Research: Space Physics*, *122*, 280–292. <https://doi.org/10.1002/2016JA023368>
- Trauger, J. T., Clarke, J. T., Ballester, G. E., Evans, R. W., Burrows, C. J., Crisp, D., et al. (1998). Saturn's hydrogen aurora: Wide field and planetary camera 2 imaging from the Hubble Space Telescope. *Journal of Geophysical Research*, *103*(E9), 20,237–20,244. <https://doi.org/10.1029/98JE01324>
- Vasyliūnas, V. M. (1983). *Physics of the Jovian magnetosphere, chap. Plasma distribution and flow* (pp. 395–453). New York: Cambridge Univ. Press.
- Yao, Z. H., Grodent, D., Ray, L. C., Rae, I. J., Coates, A. J., Pu, Z. Y., et al. (2017). Two fundamentally different drivers of dipolarizations at Saturn. *Journal of Geophysical Research: Space Physics*, *122*, 4348–4356. <https://doi.org/10.1002/2017JA024060>
- Yao, Z., Pu, Z. Y., Rae, I. J., Radioti, A., & Kubyshkina, M. V. (2017). Auroral streamer and its role in driving wave-like pre-onset aurora. *Geoscience Letters*, *4*, 8. <https://doi.org/10.1186/s40562-017-0075-6>
- Zesta, E., Lyons, L. R., & Donovan, E. (2000). The auroral signature of earthward flow bursts observed in the magnetotail. *Geophysical Research Letters*, *27*(20), 3241–3244. <https://doi.org/10.1029/2000GL000027>
- Zhu, L., Schunk, R., & Sojka, J. (1997). Polar cap arcs: A review. *Journal of Atmospheric and Solar-Terrestrial Physics*, *59*(10), 1087–1126. [https://doi.org/10.1016/s1364-6826\(96\)00113-7](https://doi.org/10.1016/s1364-6826(96)00113-7)